The partition function of interfaces from the Nambu-Goto effective string theory

To cite this article: Marco Billó *et al* JHEP02(2006)070

View the article online for updates and enhancements.

The partition function of interfaces from the Nambu-Goto effective string theory[*]

Marco Billó, Michele Caselle and Livia Ferro

Dipartimento di Fisica Teorica, Università di Torino
and Istituto Nazionale di Fisica Nucleare — sezione di Torino
Via P. Giuria 1, I-10125 Torino, Italy
E-mail: `billo@to.infn.it`, `caselle@to.infn.it`, `ferro@to.infn.it`

ABSTRACT: We consider the Nambu-Goto bosonic string model as a description of the physics of interfaces. By using the standard covariant quantization of the bosonic string, we derive an exact expression for the partition function in dependence of the geometry of the interface. Our expression, obtained by operatorial methods, resums the loop expansion of the NG model in the "physical gauge" computed perturbatively by functional integral methods in the literature. Recently, very accurate Monte Carlo data for the interface free energy in the 3d Ising model became available. Our proposed expression compares very well to the data for values of the area sufficiently large in terms of the inverse string tension. This pattern is expected on theoretical grounds and agrees with previous analyses of other observables in the Ising model.

KEYWORDS: Bosonic Strings, Confinement, Lattice Gauge Field Theories.

Contents

1. Introduction

The idea that string theory may provide the effective description of confining gauge theories in their strong-coupling regime is an old and well motivated one [1 – 3]; in this context, the string degrees of freedom describe the fluctuations of the colour flux tube.

In the last years much effort has been devoted to test this conjecture. In particular, several results have been obtained in an "effective string" approach, in which the conformal anomaly due to the fact that the theory is quantized in a non-critical value $d \neq 26$ of the space-time dimensionality is neglected. In principle, this is a very problematic simplification, since conformal invariance is at the very heart of the quantization procedure (see the Conclusions section for some remarks on this issue). However, it was observed very early [4] that the coefficient of the conformal anomaly vanishes for large distances, i.e., for world-sheets of large size in target space. In fact, in recent years, thanks to various improvements in lattice simulations [5 – 8] the effective string picture has been tested with a very high precision and confidence [8]-[28] by considering observables such as Wilson loops and Polyakov loop correlators. It turns out that at large inter-quark distances and low temperatures the effective string, and in particular the simplest model, the Nambu-Goto one, correctly describes the Monte Carlo data. As distances are decreased, clear deviations from this picture are observed [11, 13, 17, 18].

Within the effective string framework, one can fix a "physical gauge" (see section 1.2 for some more details) and re-express a generic effective string model as a 2d (interacting) conformal field theory of $d-2$ bosons. In this set-up, the inverse of the product of the string tension σ times the minimal area $\mathcal{A}$ of the world sheet spanned by the string represents the parameter of a loop expansion around the classical solution for the inter-quark potential. The first term of this expansion yields the well known Lüscher correction [2]. The second term was evaluated more than twenty years ago in [29], with a remarkable theoretical effort, for several different classes of effective string actions. Higher order corrections would require very complicated calculations and have never appeared in the literature.

Recently, a set of simulations both in SU(2) and SU(3) lattice gauge theories (LGT's) [9, 10, 12, 17, 18, 20 – 22, 24] and in the 3d gauge Ising model [6, 8, 11, 13, 14], thanks to powerful new algorithms, estimated the inter-quark potential with precision high enough to distinguish among different effective string actions and to observe the contribution of higher string modes. To compare the effective string predictions with these new data in a meaningful way it is mandatory to go beyond the perturbative expansion.

So far this has been done only for the simplest effective string action, the Nambu-Goto one [30], and for the cylindric geometry, which physically corresponds to the expectation value of the correlator of two Polyakov loops. In this case it has been possible to build the partition function corresponding to the spectrum of the Nambu-Goto string with the appropriate boundary conditions derived long ago in [31, 32], and to make a successfull comparison with the simulations [13, 14]. In [33] this partition function was re-derived via standard covariant quantization, showing that it indeed represents the exact operatorial result which re-sums the loop expansion of the model in the physical gauge.

As a further step in this direction we derive in the present paper the exact partition function of the Nambu-Goto effective string for a toroidal world-sheet geometry, and we compare this prediction to a set of recently published [34] high precision Monte Carlo results for the corresponding observable in the 3d gauge Ising model, namely the interface expectation value.

Indeed, the toroidal geometry corresponds in LGT's to the "maximal 't Hooft loop" (see, for instance, [15, 16]). However a much simpler, yet physically very interesting, observable can be associated to the same geometry if we consider a three-dimensional LGT with a discrete abelian gauge group (like the 3d gauge Ising model). In this case the gauge model is mapped by duality into a three-dimensional spin model (like the 3d spin Ising model). In particular, the confining regime of the gauge model is mapped into the broken symmetry phase of the spin model. Any extended gauge observable, like the Wilson loop or the correlator of two Polyakov loops, is mapped into a set of suitably chosen anti-ferromagnetic bonds. The torus geometry we are interested in corresponds to the case in which the set of anti-ferromagnetic bonds pierces a complete slice of the lattice, i.e., to the case in which we simply impose anti-periodic boundary conditions in one of the lattice directions. In a spin model with discrete symmetry group this type of boundary conditions is known to create, in the broken symmetry phase, an interface between two different vacua. The (logarithm of the) expectation value of the slice of anti-ferromagnetic bonds, which we expect to be described by the Nambu-Goto string, is thus proportional to

the interface free energy, an observable which has been the subject of several numerical and experimental studies in condensed matter literature. We shall briefly recall these results in section 1.1.

To compute the partition function, we follow the philosophy of [33] and resort to standard covariant quantization in the first order formulation of the Nambu-Goto theory, of which we briefly recall some aspects in section 1.2. In section 2 we integrate appropriate sectors of the bosonic string partition function over the world-sheet modular parameter. In this way we describe in an exact manner the string fluctuations around a specified target space surface, in our case representing an interface in a compact space. In section 3 we show that our expression reproduces the result obtained in [29] via a perturbative expansion (up to two loops) of the NG functional integral; in fact, our expression re-sums the loop expansion.

In section 4 we compare our predictions with the data for the free energy of interfaces in the 3d Ising presented in [34]. Our NG prediction agrees remarkably to the data for values of the area larger than (approximately) four times the inverse string tension, which is the same distance scale below which deviations from the NG model emerged in the studies of other observables cited above [13]. In the range where there is agreement, we find that the NG result is largely dominated by the lowest level mode of the bosonic string; the free energy associated to this mode already accounts very well for the MC data, apart from a shift of the overall normalization. Though corresponding to a single particle mode, this contribution is essentially stringy, since this mode pertains to a wrapped string.

1.1 Interfaces and effective strings

The properties of interfaces in three-dimensional statistical systems have been a long-standing subject of research. In particular the interest of people working in the subject has been attracted by the so called "fluid" interfaces whose dynamics is dominated by massless excitations (for a review see for instance [35, 36]). For this class of interfaces, thanks to the presence of long range massless modes, microscopic details such as the lattice structure of the spin model or the chemical composition of the components of the binary mixture become irrelevant and the physics can be rather accurately described by field theoretic methods.

An effective model widely used to describe a rough interface is the *capillary wave model* (CWM) [37, 38]. Actually this model (which was proposed well before the Nambu-Goto papers) exactly coincides [36] with the Nambu-Goto one, since it assumes an effective Hamiltonian proportional to the variation of the area of the surface with respect to the classical solution.

A simple realization of fluid interfaces is represented by 3d spin models. In the broken-symmetry phase at low temperature, these models admit different vacua which, for a suitable choice of the boundary conditions, can occupy macroscopic regions and are separated by domain walls which behave as interfaces. For temperatures between the roughening and the critical one, interfaces are dominated by long wavelength fluctuations (i.e. they exactly behave as *fluid* interfaces); all the simulations which we shall discuss below were performed in this region.

In these last years the 3d Ising model has played a prominent role among the various realizations of fluid interfaces, for several reasons. The universality class of the Ising model includes many physical systems, ranging from binary mixtures to amphiphilic membranes. Its universality class is also the same of the ϕ^4 theory; this allows a QFT approach to the description of the interface physics [39 – 41]. Last but not least, the Ising model, due to its intrinsic simplicity, allows fast and high statistics Monte Carlo simulations, so that very precise comparisons can be made between theoretical predictions and numerical results.

Following this line, during the past years some high precision tests of the capillary wave model were performed [42, 43, 34]. A remarkable agreement was found between the numerical results for interfaces of large enough size and the next to leading order approximation of the CWM. The present paper represents a further step in this direction, since we shall be able to compare the numerical data of [34] with the exact prediction of the Nambu-Goto effective model for the interface free energy.

1.2 The Nambu-Goto model

Perhaps the most natural model to describe fluctuating surfaces is the Nambu-Goto bosonic string [30], in which the action is proportional, via the string tension σ, to the induced area of a surface embedded in a d-dimensional target space:

$$S = \sigma \int d^2\xi \sqrt{\det g} \, , \qquad g_{\alpha\beta} = \frac{\partial X^i}{\partial \xi^\alpha} \frac{\partial X^j}{\partial \xi^\beta} G_{ij} \, . \tag{1.1}$$

Here we parametrize the surface by proper coordinates ξ^α, and $X^i(\xi)$ $(i = 1, \ldots, d)$ describes the target space position of a point specified by ξ. For us the target space metric G_{ij} will always be the flat one.

The invariance under re-parametrizations of the action (1.1) can be used to fix a so-called "static" gauge where the proper coordinates are identified with two of the target space coordinates, say X^0 and X^1. The quantum version of the NG theory can then be defined through the functional integration over the $d - 2$ transverse d.o.f. $\vec{X}(X^0, X^1)$ of the gauge-fixed action. The partition function for a surface Σ with prescribed boundary conditions is given by

$$
\begin{aligned}
Z_\Sigma &= \int_{(\partial\Sigma)} DX^i \exp\left\{ -\sigma \int_\Sigma dX^0 dX^1 \left(1 + (\partial_0\vec{X})^2 + (\partial_1\vec{X})^2 + (\partial_0\vec{X} \wedge \partial_1\vec{X})^2 \right)^{\frac{1}{2}} \right\} \\
&= \int_{(\partial\Sigma)} DX^i \exp\left\{ -\sigma \int_\Sigma dX^0 dX^1 \left[1 + \frac{1}{2}(\partial_0\vec{X})^2 + \frac{1}{2}(\partial_1\vec{X})^2 + \text{interactions} \right] \right\} \, .
\end{aligned}
\tag{1.2}
$$

Expanding the square root as in the second line above, the classical area law $\exp(-\sigma\mathcal{A})$ (where $\mathcal{A}$ is the area of the minimal surface Σ) is singled out. It multiplies the quantum fluctuations of the fields $\vec{X}$, which have a series of higher order (derivative) interactions. The functional integration can be performed perturbatively, the loop expansion parameter being $1/(\sigma\mathcal{A})$, and it depends on the boundary conditions imposed on the fields $\vec{X}$, i.e., on the topology of the boundary $\partial\Sigma$ and hence of Σ. The cases in which Σ is a disk, a cylinder or a torus are the ones relevant for an effective string description of, respectively, Wilson loops, Polyakov loop correlators and interfaces in a compact target space.

The computation was carried out up to two loops in [29], see also [42, 44]. The surface Σ is taken to be a rectangle, with the opposite sides in none, one or both directions being identified to get the disk, the cylinder or the torus topology. At each loop order, the result depends in a very non-trivial way on the geometry of Σ, namely on its area $\mathcal{A}$ and on the ratio u of its two sides: it typically involves non-trivial modular forms of the latter. The two loop result for the case of interfaces is reported here in section 3.

An alternative treatment of the NG model, which is the standard one described in most textbooks on string theory, see for instance [45], takes advantage of the first order formulation, in which the action is simply

$$S = \sigma \int d\xi^0 \int_0^{2\pi} d\xi^1 \, h^{\alpha\beta} \partial_\alpha X^i \partial_\beta X^i \; . \tag{1.3}$$

Here $h_{\alpha\beta}$ is an independent world-sheet metric, $\xi^1 \in [0, 2\pi]$ parametrizes the spatial extension of the string and ξ^0 its proper time evolution. Integrating out h, we retrieve the NG action eq. (1.1).

As it is well known, to include the process of splitting and joining of strings, i.e., to include string interactions, one must consider world-sheets of different topology, i.e., Riemann surfaces of different genus g. The genus of the world-sheet represents thus the loop order in a "string loop" expansion. For each fixed topology of the world-sheet, instead of integrating out h, we can use re-parametrization and Weyl invariance to put the metric in a reference form $e^\phi \hat{h}_{\alpha\beta}$ (conformal gauge fixing). For instance, on the sphere, i.e. at genus $g = 0$, we can choose $\hat{h}_{\alpha\beta} = \eta_{\alpha\beta}$, while on the torus, at genus $g = 1$, $\hat{h}_{\alpha\beta}$ is constant, but still depends on a single complex parameter τ, the modulus of the torus; see later for some more details. The scale factor e^ϕ decouples at the classical level[1] and the action takes then the form

$$S = \sigma \int d\xi^0 \int_0^{2\pi} d\xi^1 \, \hat{h}^{\alpha\beta} \partial_\alpha X^i \partial_\beta X^i + S_{\text{gh.}} \; , \tag{1.4}$$

where $S_{\text{gh.}}$ in eq. (1.3) is the action for the ghost and anti-ghost fields (traditionally called c and b) that arise from the Jacobian to fix the conformal gauge; we do not really need its explicit expression here, see [47] or [45] for reviews. The modes of the Virasoro constraints $T_{\alpha\beta} = 0$, which follow from the $h^{\alpha\beta}$ equations of motion, generate the residual conformal invariance of the model. The ghost system corresponds to a CFT of central charge $c_{\text{gh.}} = -26$. The fields $X^i(\tau, \sigma)$, with $i = 1, \ldots, d$, describe the embedding of the string world-sheet in the target space and form the simple, well-known two-dimensional CFT of d free bosons.

2. The partition function for the interface from bosonic strings

In the present section we want to describe the fluctuations of an interface in a toroidal

---

[1]Actually, this property persists at the quantum level only if the anomaly parametrized by the total central charge $c = d - 26$ vanishes; Weyl invariance is otherwise broken and the mode ϕ, as shown by Polyakov long ago [46], has to be thought of as a field with a Liouville-type action. However, as argued in the Introduction and in the Conclusions section, we can, in first instance, neglect this effect for our purposes.

target space T^d by means of standard closed bosonic string theory. We use the standard first order formulation discussed in section 1.2 and we specify the periodicity of the target space coordinates to be $x^i \sim x^i + L^i$ $(i = 1, \ldots, d)$.

The partition function for the bosonic string on the target torus T^d is expressed as

$$\mathcal{Z}^{(d)} = \int \frac{d^2\tau}{\tau_2} \, Z^{(d)}(q, \bar{q}) \, Z^{\text{gh}}(q, \bar{q}). \tag{2.1}$$

Here $\tau = \tau_1 + i\tau_2$ is the modular parameter of the world-sheet, which is a surface of genus $g = 1$, i.e., a torus. Moreover, $Z^{(d)}(q, \bar{q})$ is the CFT partition function of the d compact bosons X^i defined on such a world-sheet. In an operatorial formulation, this reads

$$Z^{(d)}(q, \bar{q}) = \text{Tr} \; q^{L_0 - \frac{d}{24}} \, \bar{q}^{\tilde{L}_0 - \frac{d}{24}} \;, \tag{2.2}$$

where

$$q = \exp(2\pi i\tau) \;, \quad \bar{q} = \exp(-2\pi i\bar{\tau}) \;. \tag{2.3}$$

L_0 and $\tilde{L}_0$ (particular modes of the Virasoro constraints) are the left and right-moving dilation generators. With $Z^{\text{gh}}(q, \bar{q})$ we denote the CFT partition function for the ghost system, defined on the same world-sheet.

The modular parameter τ is the Teichmuller parameter of the world-sheet surface: as discussed in subsection 1.2, using Weyl invariance and diffeomorphisms we can choose the reference metric $\hat{h}_{\alpha\beta}$ to be constant and of unit determinant, but the complex parameter τ, with $\text{Im}\tau \geq 0$, which characterizes the complex structure, i.e., the shape of the torus, cannot be fixed. It is thus necessary to integrate over it, as indicated in eq. (2.1), the integration domain[2] being the upper half-plane. In the Polyakov approach [46], this integration is the remnant of the functional integration over the independent world-sheet metric $h_{\alpha\beta}$ after the invariances of the model have been used as described above. The measure used in eq. (2.1) ensures, as we will see, the modular invariance of the integrand.

The CFT partition function for a single boson defined on a circle

$$X(\xi^0, \xi^1) \sim X(\xi^0, \xi^1) + L \tag{2.4}$$

is given, with the action defined as in eq. (1.4), by[3]

$$Z(q, \bar{q}) = \text{Tr} \; q^{L_0 - \frac{d}{24}} \, \bar{q}^{\tilde{L}_0 - \frac{d}{24}} = \sum_{n,w \in \mathbb{Z}} q^{\frac{1}{8\pi\sigma}\left(\frac{2\pi n}{L} + \sigma wL\right)^2} \bar{q}^{\frac{1}{8\pi\sigma}\left(\frac{2\pi n}{L} - \sigma wL\right)^2} \frac{1}{\eta(q)} \frac{1}{\eta(\bar{q})} \;. \tag{2.5}$$

The integers n and w are zero-modes of the field X, describing respectively its discrete momentum $p = 2\pi n/L$ and its winding around the compact target space: X must be periodic in ξ^1, but the target space identification eq. (2.4) allows the possibility that

$$X(\xi^0, \xi^1 + 2\pi) = X(\xi^0, \xi^1) + wL \;. \tag{2.6}$$

---

[2]We will discuss later the issue of discrete modular transformations acting on τ.

[3]With an abuse of notation, and for the sake of convenience, we will sometimes denote the Dedekind eta function $\eta(\tau)$ defined in eq. (C.1) as $\eta(q)$, where $q = \exp(2\pi i\tau)$.

The factors of $1/\eta(q)$ and $1/\eta(\bar{q})$ result from the trace over the left and right moving non-zero modes, which after canonical quantization become just bosonic oscillators contributing to L_0 and $\tilde{L}_0$ their total occupation numbers.

The Hamiltonian trace eq. (2.5) can be re-summed á la Poisson, see eq. (C.10), over the integer n, after which it becomes

$$Z(q,\bar{q}) = \sqrt{\frac{\sigma}{2\pi}} L \sum_{m,w\in\mathbb{Z}} e^{-\frac{\sigma L^2}{2\tau_2}|m-\tau w|^2} \frac{1}{\sqrt{\tau_2}\eta(q)\eta(\bar{q})} \ , \tag{2.7}$$

an expression which is naturally obtained from the path-integral formulation. The discrete sum over m, w represents the sum over "world-sheet instantons", namely classical solutions of the field X which, beside their wrapping number w over the ξ^1 direction, are characterized also by their wrapping m along the compact propagation direction:

$$X(\xi^0 + 2\pi\tau_2, \xi^1 + 2\pi\tau_1) = X(\xi^0, \xi^1) + mL \ . \tag{2.8}$$

The form eq. (2.7) of $Z(q,\bar{q})$ makes its modular invariance manifest. In fact, the combination $\sqrt{\tau_2}\eta(q)\eta(\bar{q})$ is modular invariant, as it follows from the properties of the Dedekind eta function given in eq. (C.4). Moreover, from the exponential term we infer the effect of modular transformations of the parameter τ on the wrapping integers w, m: they act as $\mathrm{SL}(2,\mathbb{Z})$ matrices on the vector (m, w). In particular, the S and T generators of the modular group are represented as follows:

$$S: \qquad \tau \to -\frac{1}{\tau} \ , \qquad\qquad \begin{pmatrix} m \\ w \end{pmatrix} \to \begin{pmatrix} 0 & -1 \\ 1 & 0 \end{pmatrix} \begin{pmatrix} m \\ w \end{pmatrix} \ , \tag{2.9}$$

$$T: \qquad \tau \to \tau + 1 \ , \qquad\qquad \begin{pmatrix} m \\ w \end{pmatrix} \to \begin{pmatrix} 1 & -1 \\ 0 & 1 \end{pmatrix} \begin{pmatrix} m \\ w \end{pmatrix} \ . \tag{2.10}$$

This allows to reabsorb the effect of modular transformations by relabelling the sums over m and w.

The partition function for the ghost system is given by

$$Z^{\mathrm{gh}}(q,\bar{q}) = (\eta(q)\eta(\bar{q}))^2 \ , \tag{2.11}$$

namely it coincides with the inverse of the non zero-mode contributions of two bosons. Notice that the string partition function eq. (2.1) can be rewritten, substituting the above expression for $Z^{\mathrm{gh}}(q,\bar{q})$, in an explicitly modular-invariant way:

$$\mathcal{Z}^{(d)} = \int \frac{d^2\tau}{(\tau_2)^2} \left(\sqrt{\tau_2}\eta(q)\eta(\bar{q})\right)^2 Z^{(d)}(q,\bar{q}) \ , \tag{2.12}$$

so that the integration over the modular parameter τ in eq. (2.12) has to be restricted to the fundamental cell of the modular group. Indeed, the Poincaré measure $d^2\tau/(\tau_2)^2$ and the combination $\sqrt{\tau_2}\eta(q)\eta(\bar{q})$ are modular invariant. The bosonic partition function $Z^{(d)}(q,\bar{q})$ is also modular invariant, being the product of d expressions of the type eq. (2.5). It depends on integers n^i and w^i, the discrete momentum and winding number for each
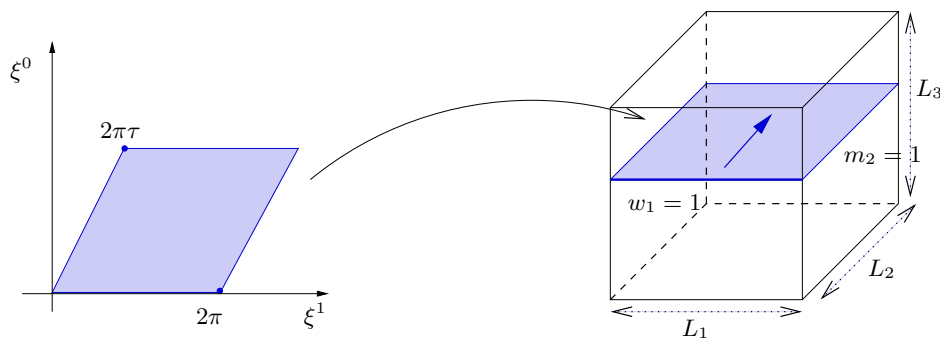
Figure 1: The mapping of the toroidal string world-sheet, of modular parameter τ, into the target space is organized in many distinct sectors, labeled by the integers w_i and m_i (see the text). By selecting the sector with (say) $w_1 = 1$ and $m_2 = 1$ we are considering the fluctuations of an extended interface, which is a torus because of the target space periodicity.
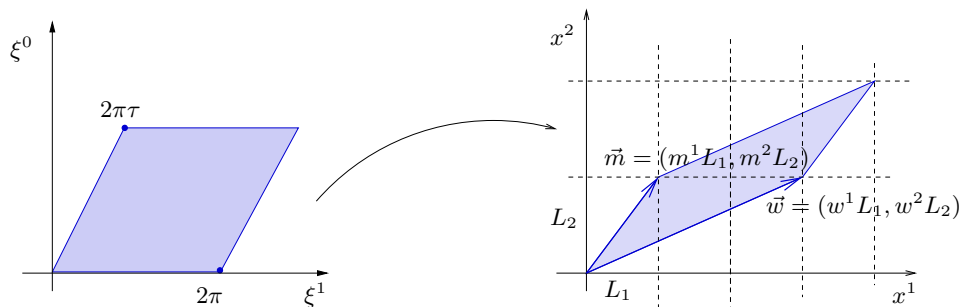

Figure 2: Consider an embedding of the world-sheet torus into the target space T^2 aligned along the directions x^1, x^2, characterized by the wrapping numbers (m^1, w^1) and (m^2, w^2). It corresponds, in the covering space of this T^2, to a parallelogram defined by the vectors $\vec{w} = (w^1 L_1, w^2 L_2)$ and $\vec{m} = (m^1 L_1, m^2 L_2)$, whose area is $\vec{w} \wedge \vec{m} = L_1 L_2 (w^1 m^2 - w^2 m^1)$.

direction. For each direction i, we can Poisson re-sum over the discrete momentum n^i, as in eq. (2.7), replacing it with the topological number m^i.

We want to single out the contributions to the partition function eq. (2.12) which describe the fluctuations of an interface aligned along a two-cycle T^2 inside T^d, say the one in the x^1, x^2 directions. The world-sheet torus parametrized by ξ^0, ξ^1 must be mapped onto the target space torus by embedding functions $X^1(\xi^0, \xi^1), X^2(\xi^0, \xi^1)$ with non-trivial wrapping numbers (m^1, w^1) and (m^2, w^2). The wrapping numbers of $X^i(\xi^0, \xi^1)$, $i > 2$, must instead vanish. The minimal area spanned by such a wrapped torus is given by (see figure 2)

$$L_1 L_2 \left(w^1 m^2 - m^1 w^2 \right) = L_1 L_2 \begin{pmatrix} m^1 & w^1 \end{pmatrix} \begin{pmatrix} 0 & -1 \\ 1 & 0 \end{pmatrix} \begin{pmatrix} m^2 \\ w^2 \end{pmatrix} . \tag{2.13}$$

A particular sector which contributes to such a target-space configuration can be obtained (see figure 1) by considering a string winding once in, say, the x^1 direction:

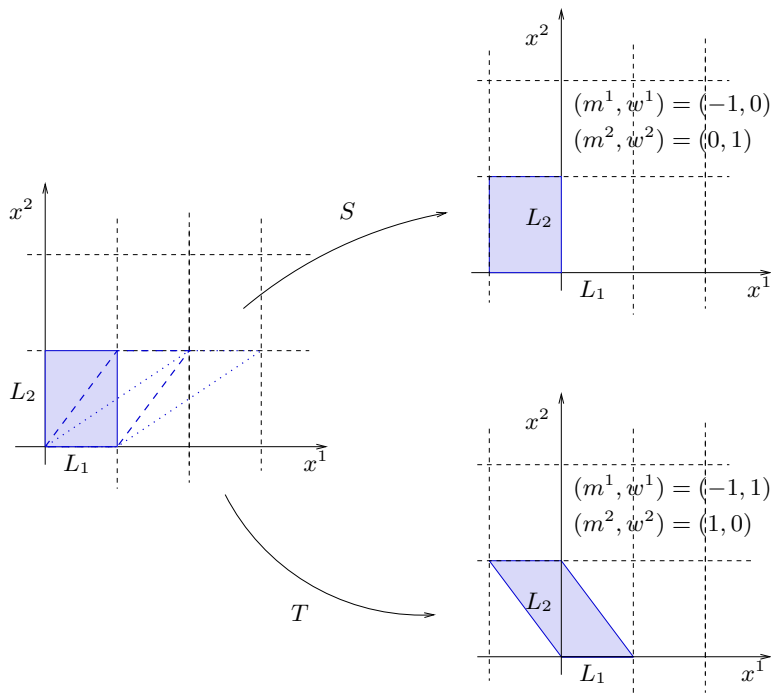$$w_1 = 1 , \quad w_2 = w_3 = \ldots = w_d = 0 \tag{2.14}$$

Figure 3: On the left, (some of) the coverings corresponding to the chosen sector of the partition function are depicted. Beside the one which exactly corresponds to the fundamental cell of the target space T^2, i.e. the case with $(m^1, w^1) = (0, 1)$ and $(m^2, w^2) = (1, 0)$ there are "slanted" ones corresponding to generic values of m^1. The generators S and T of the world-sheet modular group, which act by $\mathrm{SL}(2, \mathbb{Z})$ matrices as indicated in eq. (2.9), map these coverings to different ones with the same area. For instance, on the right, we draw the S- and T-transform of the "fundamental" covering discussed above (the solid one in the leftmost drawing).

and, upon Poisson re-summation along the directions x^2 to x^d, selecting the integers

$$ m_2 = 1 , \quad m_3 = m_4 = \ldots = m_d = 0 . \tag{2.15} $$

This corresponds to wrapping numbers in the x^1, x^2 directions given by $(m^1, w^1) = (m^1, 1)$ and $(m^2, w^2) = (1, 0)$ and hence, according to eq. (2.13), to a minimal area $L_1 L_2$: such a configuration covers the two-cycle in the x^1, x^2 directions just once. We have not fixed the value of the wrapping number m^1, therefore the sector we consider contains infinite embeddings that corresponds to "slanted" coverings, see figure 3.

The choice $w_i = m_i = 0$ for $i = 3, \ldots, d$ is preserved under the action eq. (2.9) of the modular group. Moreover, this $\mathrm{SL}(2, \mathbb{Z})$ action preserves the area eq. (2.13), as it is easy to see[4]. The orbit of the modular group which contains the configurations chosen in eqs. (2.14)–(2.15) spans thus infinite other string configurations characterized by different wrapping numbers in the directions x^1, x^2; all these configurations, however, always wrap

---

[4]The expression of the area eq. (2.13) contains the symplectic product of the two vectors (m^1, w^1) and (m^2, w^2). The simultaneous action of $\mathrm{SL}(2, \mathbb{Z})$ on both vectors preserves this symplectic product: $\mathrm{SL}(2) \sim \mathrm{Sp}(1)$.

the T^2 in target space just once, and correspond to equivalent descriptions of the interface; see figure 3.

To obtain the partition function for this interface we should include all the wrapping numbers (m^1, w^1) and (m^2, w^2) which are in the modular orbit of the configurations in eqs. (2.14)–(2.15), but we should integrate the τ parameter in eq. (2.16) over the fundamental cell of the modular group only, as usual, to avoid overcounting. We can, equivalently, consider only the configurations of eqs. (2.14)–(2.15), fixing in this way the degeneracy associated to modular transformations, and integrate τ all over the upper half-plane, which contains all the images under modular transformations of the fundamental cell.

The second choice turns out to be convenient, as the integrals become very simple. In this way, we get the following expression for the interface partition function:

$$
\mathcal{I}^{(d)} = \int \frac{d^2\tau}{(\tau_2)^{\frac{d+1}{2}}} \left[\frac{1}{\eta(q)} \frac{1}{\eta(\bar{q})} \right]^{d-2} \sum_{n_1 \in \mathbb{Z}} q^{\frac{1}{8\pi\sigma}\left(\frac{2\pi n_1}{L_1} + \sigma L_1\right)^2} \bar{q}^{\frac{1}{8\pi\sigma}\left(\frac{2\pi n_1}{L_1} - \sigma L_1\right)^2} \prod_{i=2}^{d} \left(\sqrt{\frac{\sigma}{2\pi}} L_i \right) \mathrm{e}^{-\frac{\sigma L_2^2}{2\tau_2}} .
$$
(2.16)

Expanding in series the Dedekind's η functions:

$$
[\eta(q)]^{2-d} = \sum_{k=0}^{\infty} c_k q^{k - \frac{d-2}{24}} ,
$$
(2.17)

and expressing q and $\bar{q}$ in terms of τ, we rewrite eq. (2.16) as

$$
\mathcal{I}^{(d)} = \prod_{i=2}^{d} \left(\sqrt{\frac{\sigma}{2\pi}} L_i \right) \sum_{k,k'=0}^{\infty} \sum_{n_1 \in \mathbb{Z}} c_k c_{k'} \int_{-\infty}^{\infty} d\tau_1 \mathrm{e}^{2\pi \mathrm{i}(k - k' + n_1)} \int_0^{\infty} \frac{d\tau_2}{(\tau_2)^{\frac{d+1}{2}}}
$$
$$
\times \exp\left\{ -\tau_2 \left[\frac{\sigma L_1^2}{2} + \frac{2\pi^2 n_1^2}{\sigma L_1^2} + 2\pi\left(k + k' - \frac{d-2}{12}\right) \right] - \frac{1}{\tau_2} \left[\frac{\sigma L_2^2}{2} \right] \right\} .
$$
(2.18)

The integration over τ_2 can be carried out in terms of modified Bessel functions using the formula

$$
\int_0^{\infty} \frac{d\tau_2}{\tau_2^{\frac{d+1}{2}}} \exp\left\{ -A^2 \tau_2 - \frac{B^2}{\tau_2} \right\} = 2 \left(\frac{A}{B} \right)^{\frac{d-1}{2}} K_{\frac{d-1}{2}}(2AB) ,
$$
(2.19)

with

$$
A = \sqrt{\frac{\sigma}{2}} L_1 \mathcal{E} , \quad B = \sqrt{\frac{\sigma}{2}} L_2
$$
(2.20)

and

$$
\mathcal{E} = \sqrt{1 + \frac{4\pi}{\sigma L_1^2}\left(k + k' - \frac{d-2}{12}\right) + \frac{4\pi^2 n_1^2}{\sigma^2 L_1^4}} = \sqrt{1 + \frac{4\pi u}{\sigma \mathcal{A}}\left(k + k' - \frac{d-2}{12}\right) + \frac{4\pi^2 u^2 n_1^2}{(\sigma \mathcal{A})^2}} .
$$
(2.21)

In the second step, we introduced the area $\mathcal{A}$ and the modular parameter $\mathrm{i}u$ of the torus swept out by the string in the target space, namely the interface:

$$
\mathcal{A} = L_1 L_2 , \quad u = \frac{L_2}{L_1} .
$$
(2.22)

The integration over τ_1 produces a $\delta(k-k'+n_1)$ factor, and thus, using eqs. 2.19–2.20, we rewrite the interface partition function eq. (2.18) as

$$\mathcal{I}^{(d)} = 2 \left(\frac{\sigma}{2\pi}\right)^{\frac{d-2}{2}} V_T \sqrt{\sigma \mathcal{A} u} \sum_{k,k'=0}^{\infty} c_k c_{k'} \left(\frac{\mathcal{E}}{u}\right)^{\frac{d-1}{2}} K_{\frac{d-1}{2}}(\sigma \mathcal{A} \mathcal{E}) \ , \qquad (2.23)$$

where $\mathcal{E}$, introduced in eq. (2.21), is now to be written replacing $k-k'$ for n_1. In eq. (2.23) we have introduced the transverse volume $V_T = \prod_{i=3}^{d} L_i$, and we have re-written the prefactor $\sqrt{\sigma} L_2$ as $\sqrt{\sigma \mathcal{A} u}$.

Eq. (2.23) gives the exact expression for the fluctuations of the interface aligned along the x^1, x^2 directions, in our hypothesis that they be described from standard bosonic string theory. This expression depends only on the target space geometric data, namely the transverse volume V_T and the area $\mathcal{A}$ and the shape parameter u of the interface.

Considering the leading exponential behaviour of the Bessel functions only, eq. (2.23) would reduce to a partition function constructed by summing over closed string states, characterized by the left- and right-moving occupation numbers k and k' and by the momentum n_1 which is fixed to $k-k'$ by the level-matching condition, with the usual bosonic multiplicities c_k, $c_{k'}$ and with exponential weights $\exp(-L_2 E_{k,k'})$, where the energies are given by

$$E_{k,k'} = \sigma L_1 \mathcal{E} = \sqrt{\sigma^2 L_1^2 + 4\pi\sigma(k+k'-\frac{d-2}{12}) + \frac{4\pi^2 n_1^2}{L_1^2}} \ . \qquad (2.24)$$

This spectrum substantially agrees with the expression proposed in [48]; however, the correct expression of the partition function, eq. (2.23), involves Bessel functions rather than exponentials and it also contains extra factors of $\mathcal{E}$. These modifications are crucial in reproducing correctly the loop expansion of the functional approach, as we shall see in the next section.

3. Comparison with the functional integral approach

As discussed in the Introduction, the Nambu-Goto interface partition function, whose expression eq. (4.3) we derived by operatorial methods in the first-order formalism, can also be computed in a functional integral approach with a physical gauge-fixing. This leaves just the $d-2$ bosonic d.o.f. corresponding to the transverse fluctuations of the interface, but the action is not a free one. One can evaluate the path integral perturbatively, the loop expansion parameter being the inverse of $\sigma \mathcal{A}$ [29]. The result of this computation up to the 2-d loop order was given in [29] and reads

$$\mathcal{I}^{(d)} \propto \sigma^{\frac{d-2}{2}} \frac{\mathrm{e}^{-\sigma \mathcal{A}}}{[\sqrt{u}\eta^2(\mathrm{i}u)]^{d-2}} \left\{ 1 + \frac{f_1(u)}{\sigma \mathcal{A}} + \dots \right\} \ . \qquad (3.1)$$

where the dots stand for higher loop contributions and

$$f_1(u) = \frac{(d-2)^2}{2} \left[\left(\frac{\pi}{6}\right)^2 u^2 E_2^2(\mathrm{i}u) - \frac{\pi}{6} E_2(\mathrm{i}u) \right] + \frac{d(d-2)}{8} \ . \qquad (3.2)$$

Here E_2 denotes the 2nd Eisenstein series (see Appendix C). Actually, the constant term in eq. (3.2) is different from the one given in [29]; in Appendix B we show, by reconsidering the computation of the second loop term, that in fact the correct result is the one we quote in eq. (3.2)[5]

Our exact expression eq. (2.23) should reproduce the perturbative expansion of the functional integral result when asymptotically expanded for large $\sigma\mathcal{A}$. To this effect, let us re-organize eq. (2.23) in a suitable way. Using the asymptotic expansion of Bessel functions for large arguments:

$$K_j(z) \sim \sqrt{\frac{\pi}{2z}} \mathrm{e}^{-z} \left(1 + \sum_{r=1}^{\infty} a_r^{(j)} z^{-r}\right) \, , \tag{3.3}$$

where the coefficients $a_r^{(j)}$ are well known, we obtain

$$\mathcal{I}^{(d)} = \sqrt{2\pi} \left(\frac{\sigma}{2\pi}\right)^{\frac{d-2}{2}} V_T \sum_{k,k'=0}^{\infty} c_k c_{k'} \left(\frac{\mathcal{E}}{u}\right)^{\frac{d-2}{2}} \mathrm{e}^{-\sigma\mathcal{A}\mathcal{E}} \left(1 + \sum_{r=1}^{\infty} a_r^{(\frac{d-1}{2})}(\sigma\mathcal{A}\mathcal{E})^{-r}\right) \, . \tag{3.4}$$

We can then Taylor expand the expression eq. (2.21) of $\mathcal{E}$ and write it in the form

$$\mathcal{E} = 1 + \sum_{t=1}^{\infty} d_t\,(a,b;u)\,(\sigma\mathcal{A})^{-t} \, , \tag{3.5}$$

having introduced, for notational simplicity,

$$a = k + k' - \frac{d-2}{12} \, , \quad b = k - k' \, . \tag{3.6}$$

In particular one has

$$d_1 = 2\pi u a = 2\pi u \left(k + k' - \frac{d-2}{12}\right) \, . \tag{3.7}$$

For the sake of readability, we leave to Appendix A most of the details of the present computation, such as explicit expressions of the various expansion coefficients, describing here only the basic steps.

Plugging the expansion eq. (3.5) into eq. (3.4) we obtain

$$\mathcal{I}^{(d)} \propto \sigma^{\frac{d-2}{2}} \frac{\mathrm{e}^{-\sigma\mathcal{A}}}{u^{\frac{d-2}{2}}} \sum_{k,k'=0}^{\infty} c_k c_{k'} \mathrm{e}^{-2\pi u\left(k+k'-\frac{d-2}{12}\right)} \left\{1 + \sum_{s=1}^{\infty} \frac{g_s\,(a,b;u)}{(\sigma\mathcal{A})^s}\right\} \, , \tag{3.8}$$

where the coefficients g_s can be re-constructed starting from the coefficients appearing in eqs. (3.3) and (3.5); see Appendix A for more details.

We can introduce $Q = \exp(-2\pi u)$ and re-write eq. (3.8) as follows:

$$\mathcal{I}^{(d)} \propto \sigma^{\frac{d-2}{2}} \frac{\mathrm{e}^{-\sigma\mathcal{A}}}{u^{\frac{d-2}{2}}} \lim_{\overline{Q}\to Q} \sum_{k,k'=0}^{\infty} c_k c_{k'} \left\{1 + \sum_{s=1}^{\infty} \frac{g_s(a,b;u)}{(\sigma\mathcal{A})^s}\right\} Q^{k-\frac{d-2}{24}} \overline{Q}^{k'-\frac{d-2}{24}} \, . \tag{3.9}$$

---

[5]It is interesting to observe that the missing contribution in [29] is proportional to $(d-3)$ and thus disappears in three dimensions. This is the reason for which it was not found in the calculations reported in [42, 44] which evaluated this 2 loop correction with three other types of regularization in the $d=3$ case. Moreover the difference is modular invariant and thus it could not be detected by Dietz and Filk in the tests of their calculation which they made in [29].

At this point, we can effectively replace

$$a = k + k' - \frac{d-2}{12} \longrightarrow Q\frac{d}{dQ} + \overline{Q}\frac{d}{d\overline{Q}} \ , \qquad b = k - k' \longrightarrow Q\frac{d}{dQ} - \overline{Q}\frac{d}{d\overline{Q}} \qquad (3.10)$$

and take into account the definition, eq. (2.17), of the coefficients c_k to obtain the form

$$\mathcal{I}^{(d)} \propto \sigma^{\frac{d-2}{2}} \frac{e^{-\sigma\mathcal{A}}}{u^{\frac{d-2}{2}}} \lim_{\overline{Q} \to Q} \left\{ 1 + \sum_{s=1}^{\infty} \frac{g_s\left(Q\frac{d}{dQ} - \overline{Q}\frac{d}{d\overline{Q}}, Q\frac{d}{dQ} + \overline{Q}\frac{d}{d\overline{Q}}; u\right)}{(\sigma\mathcal{A})^s} \right\} \left[\eta(Q)\eta(\overline{Q})\right]^{2-d} \ , \tag{3.11}$$

with, in the end, Q being set to $\exp(-2\pi u)$. Finally, we can rewrite the above expression as

$$\mathcal{I}^{(d)} \propto \sigma^{\frac{d-2}{2}} \frac{e^{-\sigma\mathcal{A}}}{[\sqrt{u}\eta^2(iu)]^{d-2}} \left\{ 1 + \sum_{s=1}^{\infty} \frac{f_s(u)}{(\sigma\mathcal{A})^s} \right\} \tag{3.12}$$

where the coefficients f_s are given by

$$f_s(u) = \eta^{2d-4}(iu) \lim_{\overline{Q} \to Q = e^{-2\pi u}} g_s\left(Q\frac{d}{dQ} - \overline{Q}\frac{d}{d\overline{Q}}, Q\frac{d}{dQ} + \overline{Q}\frac{d}{d\overline{Q}}; u\right) \left[\eta(Q)\eta(\overline{Q})\right]^{2-d} \quad (3.13)$$

and can be related to Eisenstein series. In Appendix A we derive the expression of the 2-nd loop and 3-rd loop coefficients, f_1 and f_2, but it would be straightforward to push the computation to higher orders. Our expression for f_1 agrees completely with the (corrected) Dietz-Filk result eq. (3.2). Let us remark that our result eq. (3.12) is proportional (with no need of ad hoc modifications) to $\sigma^{\frac{d-2}{2}}$, i.e. to $\sqrt{\sigma}$ in three dimensions. This result agrees with the (completely independent) field theoretical calculations in the framework of the ϕ^4 model of [39, 40] and also, as we shall see, with the Monte Carlo simulations.

4. Comparison with Monte Carlo data

In a very recent publication [34], precise Monte Carlo data on the free energy F_s of interfaces in the 3d Ising model were presented. The most accurate sets of data were obtained for square lattices (i.e., in the case $u = 1$), for values of the Ising coupling given by $\beta = 0.226102$ ([34, table 4]; we shall refer to this data set as the set n. 1) and $\beta = 0.236025$ ([34, table 2], set 2). The data set 1 contains 21 points, obtained at lattice sizes $L_1 = L_2 \equiv L$ ranging from $L = 10$ to $L = 30$; the 9 points in data set 2 are[6] for $L = 6$ to $L = 14$.

Previous work regarding other observables [13] has made it clear that, in appropriate regimes, the 3d Ising model can be successfully described by an effective string theory. For the two values of β which we study here very precise estimates for the string tension exist [49] (see [34, table 1]). For set 1 one has $\sigma = 0.0105241$; for set 2, $\sigma = 0.044023$. This entails that the points in data set 1 correspond to values of $\sqrt{\sigma\mathcal{A}}$ ranging from 1.02 to 3.07, while the points in data set 2 correspond to values from 1.26 to 2.94.

---

[6]We consider here only the data in [34, table 2] which, for a given value of L, are obtained with L_0, the size of the lattice in the transverse direction, being equal to $3L$, to ensure uniformity with the data set 1, which is obtained with this choice.

$L_{\min}$	$(\sqrt{\sigma\mathcal{A}})_{\min}$	$N = 100$		$N = 0$	
		$\mathcal{N}$	$\chi^2/(\text{d.o.f})$	$\mathcal{N}$	$\chi^2/(\text{d.o.f})$
Data set 1					
19	1.949	0.91957(18)	4.22	0.91413(18)	1.60
20	2.051	0.91891(22)	1.84	0.91377(22)	0.88
21	2.154	0.91836(27)	0.63	0.91344(27)	0.47
22	2.257	0.91829(33)	0.70	0.91354(33)	0.50
23	2.359	0.91797(45)	0.63	0.91339(45)	0.53
24	2.462	0.91762(57)	0.57	0.91316(57)	0.55
25	2.565	0.91715(75)	0.50	0.91279(75)	0.55
Data set 2					
9	1.888	0.91052(21)	7.22	0.90466(21)	2.22
10	2.098	0.90924(33)	2.71	0.90413(33)	1.69
11	2.308	0.90820(51)	1.12	0.90349(51)	1.33

Table 1: The fit of the NG free energy eq. (4.1) with normalization $\mathcal{N}$ to the two data set of Ref. [34], performed using only the points in [34, table 4 and 2] corresponding to lattice sizes $L \geq L_{\min}$, i.e., those with $\sqrt{\sigma\mathcal{A}} \geq (\sqrt{\sigma\mathcal{A}})_{\min}$. The reduced χ^2 becomes of order unity for $(\sqrt{\sigma\mathcal{A}})_{\min} \gtrsim 2$. The fit is performed by truncating the sum over the oscillator levels at $N = 100$ or at $N = 0$, i.e. keeping only the 0-mode contributions (last two columns).

Using the information above, it is possible to compare the MC values of the free energy F_s in data set 1 and 2 to the free energy F corresponding to our partition function eq. (2.23) (in $d = 3$, and for $u = 1$), where we factor out the transverse volume factor V_T and allow for an overall normalization $e^{-\mathcal{N}}$:

$$F = -\log\left(\frac{\mathcal{I}^{(3)}}{V_T}\right) + \mathcal{N} . \tag{4.1}$$

The constant $\mathcal{N}$ will be the only free parameter to be fitted to the data. For numerical evaluation of the free energy eq. (4.1), we re-arrange the sums appearing in eq. (2.23) using the property

$$\sum_{k,k'=0}^{\infty} c_k c_{k'} f((k - k')^2, k + k') = \sum_{m=0}^{\infty} \sum_{k=0}^{m} c_k c_{m-k} f\left((2k - m)^2, m\right) , \tag{4.2}$$

valid for any function f of the specified arguments, and write eq. (2.23) as

$$\mathcal{I}^{(d)} = 2\left(\frac{\sigma}{2\pi}\right)^{\frac{d-2}{2}} V_T \sqrt{\sigma\mathcal{A}u} \sum_{m=0}^{\infty} \sum_{k=0}^{m} c_k c_{m-k} \left(\frac{\mathcal{E}}{u}\right)^{\frac{d-1}{2}} K_{\frac{d-1}{2}}(\sigma\mathcal{A}\mathcal{E}) , \tag{4.3}$$

where $\mathcal{E}$ is now $\mathcal{E}((2k-m)^2, m)$, since we transformed the summation indices as in eq. (4.2). The integer m represents the total (left- plus right-moving) oscillator number; the contributions to the partition function from states of a given m are suppressed by exponentials of the type $\exp(-2\pi u\, m)$, as it can easily be seen from eq. (4.3) upon expanding the argument
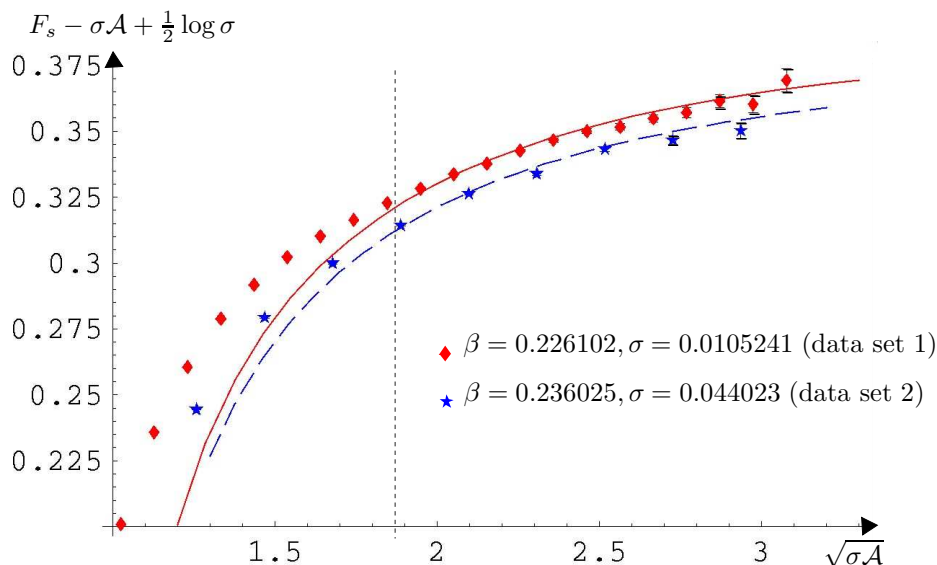
Figure 4: Two sets of Monte Carlo data for the interface free energy data provided in [34] are compared to our theoretical predictions following from eqs. (4.1), (4.3), represented by the solid line for the data set 1 and by the dashed line for data set 2. The only free parameter is the additive constant $\mathcal{N}$, corresponding to an overall normalization of the NG partition function, fitted to the data using the points to the right of the vertical dashed line (see the text for more details). The error bars in the MC data are visible only for the rightmost points, but they were kept into account in the fit. The sum over the level m in eq. (4.3) was truncated at $N = 100$.

of the Bessel function using eqs. (3.5), (3.7). We can approximate the exact expression of F by truncating the sum over m at a certain N, i.e., neglecting the contributions of string states with total occupation number larger that N.

Having fixed $u = 1$ and having specified N, the free energy F of eq. (4.1) is just a function of $\sigma\mathcal{A}$, which we can fit to the MC points in the two data sets referred to above.

The results of this comparison are summarized in table 1. For each data set, we consider only the data corresponding to lattice sizes $L \geq L_{\min}$, i.e., to values of $\sqrt{\sigma\mathcal{A}} \geq (\sqrt{\sigma\mathcal{A}})_{\min}$, and fix the value of the normalization constant $\mathcal{N}$ so as to minimize the χ^2; we repeat the analysis for various values of $L_{\min}$. Also, we consider the case where we truncate the sum over the oscillator number at $N = 100$ and the case $N = 0$ where we keep only the zero-mode contributions.

For both data sets 1 and 2, the reduced χ^2 becomes of order one when we consider in the fit only values of $\sqrt{\sigma\mathcal{A}} \gtrsim 2$. This is therefore the region in which our theoretical expression, derived from the Nambu-Goto model, describes well the data. This pattern is fully consistent with previous analysis of other observables in the 3d Ising models. In particular, the case of Polyakov loop correlators was recently discussed in [13], where two different behaviours were observed. In the compact direction corresponding to the "temperature", a good agreement with the Nambu-Goto predictions was found exactly in the same range of distances as in the present case. On the contrary, in the direction with

Dirichlet boundary conditions a clear disagreement was observed up to very large distances. This is probably due to some type of "boundary effect" associated to the Dirichlet boundary conditions. It is exactly the absence of this type of effects which makes the case that we study in the present paper, periodic in both directions and hence free of boundary corrections, particularly well suited to study the effective string contributions, disentangled from other spurious effects.

Considering the values of the χ^2, we can take as our best estimates for the normalization constant $\mathcal{N}$ the value obtained at $L_{\min} = 21$ for the data set 1, namely $\mathcal{N} = 0.9184(3)$, and the value at $L_{\min} = 11$ for data set 2, i.e. $\mathcal{N} = 0.9082(5)$. It is interesting to observe that truncating to $N = 0$ the mode expansion gives comparable values for the χ^2 but leads to a sizeable change (with respect to the statistical errors) of $\mathcal{N}$ which becomes $\mathcal{N} = 0.9134(3)$ and $\mathcal{N} = 0.9035(5)$ for the data sets 1 and 2 respectively. This difference is due to the fact that the truncation of the sum at $N = 0$ replaces the area-independent 1-loop determinant $\eta^{4-2d}(iu)$ appearing in the exact partition function eq. (3.12) with its approximation $\exp(\pi u(d-2)/6)$. This can be seen by keeping the $m = 0, k = 0$ term only in eq. (4.3), looking at the exponential behaviour $\exp(-\sigma \mathcal{A}\mathcal{E})$ and expanding $\mathcal{E}$ to the first order, see eqs. (3.5)–(3.7). In our situation, where $d = 3$ and $u = 1$, the 1-loop determinant (which is essentially reproduced summing the contributions up to $N = 100$) contributes to the free energy a constant term $2\log[\eta(i)] = -0.527344...$; in the $N = 0$ truncation, this constant becomes $-\pi/6 = -0.523599$. The difference between these two values is $0.00374536...$, and accounts for most of the difference between the estimates of the overall constant $\mathcal{N}$ at $N = 100$ and $N = 0$ given above.

It is instructive to compare our estimates for the overall constant with those obtained in [34] by truncating the perturbative expansion in $1/\sigma\mathcal{A}$ to the second order. Keeping into account the difference in the definition of the normalizations, which simply amounts to the contribution $2\log[\eta^2(i)]$ of the one-loop determinant, we would obtain, using the notations of [34], $c_0 + \frac{1}{2}\log\sigma = 0.3910(3)$ for the data set 1 and $N = 100$, which should be compared with the value $c_0 + \frac{1}{2}\log\sigma = 0.388(5)$. The estimates are compatible within the errors. Since the fit we performed depends on one free parameter only, our estimate for $c_0 + \frac{1}{2}\log\sigma$ turns out to be more precise than the one of [34]. As discussed in [34] the result we obtain is of the order of magnitude but somehow larger than the prediction obtained in [43, 39] in the framework of the ϕ^4 theory: $c_0 + \frac{1}{2}\log\sigma \sim 0.29$.

To make the above discussion visually appreciable, in figure 4 we plot our theoretical curve against the MC points, having fixed the value of the normalization $\mathcal{N}$ according to the fit at $L_{\min} = 21$ for the data set 1 and at $L_{\min} = 11$ for data set 2 and having truncated the sum over the oscillators at $N = 100$ in both cases. In fact, to draw a readable plot, it is convenient to subtract from both the Monte Carlo data and the theoretical prediction for the free energy the dominant scaling term $\sigma\mathcal{A}$ and a constant[7] term $-\frac{1}{2}\log\sigma$.

In [34, table 9] some data regarding rectangular lattices, i.e., with $u > 1$ were also

---

[7]This term is related to the natural appearance of a multiplicative factor $\sigma^{\frac{d-2}{2}}$ in the effective string partition function, see eq. (4.3). Furthermore we prefer to exhibit the same data plots appearing in [34].

L_1	L_2	$\sqrt{\sigma\mathcal{A}}$	u	F_s	diff ($N=100$)	diff ($N=0$)
10	12	2.29843	6/5	7.1670(6)	0.0016	0.0049
10	15	2.56972	3/2	8.4449(12)	-0.0004	0.0042
10	18	2.81498	9/5	9.6976(17)	-0.0009	0.0037
10	20	2.96725	2	10.5235(25)	-0.0012	0.0035
10	22	3.11208	11/5	11.3466(36)	0.0017	0.0064

Table 2: Comparison between the data presented in [34] for rectangular lattices and our predictions. The data were extracted at $\beta = 0.236025$, corresponding to $\sigma = 0.044023$, i.e., in the same situation as for the square lattices considered in data set 2 considered above. In the last columns we give the MC values of the free energy F_s, according to [34, table 9], and the difference between these values and the values obtained from our expression eq. (4.1), with the sum over the oscillator number truncated at $N = 100$ or at $N = 0$. The normalization constant $\mathcal{N}$ was already determined by the fit to the data set 2 presented in table 1; we chose here the value obtained setting $L_{\min} = 11$.

presented. Such data represent an important test of the form of our expression 4.1. We present the results of this test in table 2; they are quite encouraging, since we basically get agreement with the data within the error bars, at least when including the contributions of higher oscillator numbers (up to $N = 100$). Notice that in this test we use the value of the normalization constant $\mathcal{N}$ already determined by fitting it to the data for squared lattices of data set 2, see table 1, since the data for asymmetric lattices in ref. [34] were obtained at exactly the same value of the coupling constant β used for the data set 2. This makes the observed agreement even more remarkable, since it involved no adjustable free parameter.

It would clearly be desirable to obtain more extended sets of data for asymmetric lattices, to check their degree of consistency with our Nambu-Goto predictions.

One remarkable feature of the comparisons presented here in tables 1 and 2 is that keeping just the zero modes of the string, i.e. setting $N = 0$, seems to yield a very good agreement with the data, in particular for symmetric interfaces. The contribution of non-zero modes modifies the overall normalization coming from the one-loop determinant, as discussed above, but it is much less important for higher loops, so that the shape of the free energy as a function of $\sigma\mathcal{A}$ is little changed.

Keeping only the zero-modes, the quantity $\mathcal{E}$ of eq. (2.21) which appears in the partition function reduces effectively to

$$\widehat{\mathcal{E}} = \sqrt{1 - \frac{\pi u(d-2)}{3\sigma\mathcal{A}}} \tag{4.4}$$

and the partition function eq. (4.3) simply becomes

$$\widehat{\mathcal{I}}^{(d)} = 2\left(\frac{\sigma}{2\pi}\right)^{\frac{d-2}{2}} V_T \sqrt{\sigma\mathcal{A}u} \left(\frac{\widehat{\mathcal{E}}}{u}\right)^{\frac{d-1}{2}} K_{\frac{d-1}{2}}\left(\sigma\mathcal{A}\widehat{\mathcal{E}}\right) . \tag{4.5}$$

5. Conclusions

In this paper, we studied the free energy of interfaces in a compact d-dimensional target space T^d, modeling them with a Nambu-Goto string effective action; this basically corre-

sponds, for the $d = 3$ case, to use the capillary wave model. Performing standard covariant quantization and explicitly integrating over the modular parameter of the world-sheet, we were able to derive an exact expression for the sector of the NG partition function that describes the interface fluctuations .

Focusing on the three-dimensional case, we compared the exact predictions of the NG model with the free energy of interfaces obtained in [34] through very precise Monte Carlo simulations in the Ising model. The Monte Carlo data are very well accounted for when we consider lattices of sufficiently large sizes, typically with $L \geq 2/\sqrt{\sigma}$; here σ is the string tension, which can be associated with great accuracy to the value of the Ising coupling [49].

Our analysis, which allows to compare the data with the exact theoretical prediction, confirms and strengthens the evidence that the NG model is a very reliable effective model for such lattice sizes. Previously, comparisons were made to the two-loop expansion of the NG model [29], which already gives a very good approximation for square interfaces; as pointed out in [34], however, and as confirmed here, higher order corrections are more important for asymmetric lattices. In fact, we found extremely good agreement of the exact expression (which re-sums all the loop corrections) for the few data with $u \neq 1$ presented in [34]; it would be very interesting to obtain extended set of high precision Monte Carlo data for asymmetric lattices to check whether this agreement is confirmed, and to what extent.

For smaller lattice sizes, rather large deviations from the NG predictions are observed in the data. This pattern is in perfect agreement with what has been observed in previous studies of the NG predictions for other observables, such as the Polyakov loop correlator [13], and is in fact to be expected for deep theoretical motivations.

Indeed, we have studied the Nambu-Goto bosonic string in d dimension paying no attention to the fact that in a consistent quantum treatment, when $d \neq 26$ further degrees of freedom have to be taken into account, beside the $d - 2$ transverse oscillations. In the Polyakov first order formulation [46], the scale e^ϕ of the world-sheet metric h does not decouple, and gets in fact a Liouville-type action; in the Virasoro treatment, longitudinal modes of the string enter the game [50, 51] (the two effects are not disconnected, see [52]). For this reason these quantum bosonic string models have not been considered in the past [53, 57] as viable dual descriptions of situations, such as the confining regime of gauge theories or the fluid interfaces, where only transverse fluctuations are expected on physical grounds.

In a modern perspective, the extra degree of freedom corresponding to the Liouville mode could play somehow the rôle of the renormalization scale [54, 55], in the spirit of (a non-conformal version of) AdS/CFT duality [56]. It would be very interesting to try to take into account the contributions to the partition function of the extra d.o.f. arising in $d = 26$ at the quantum level, and to see whether they can account for the deviations of data, at small lattice sizes, from the prediction obtained via the naïve treatment of the NG model. Some effort in this direction, focusing on the relevance of the longitudinal modes for the description of large N gauge theories, has been done in [61].

In [57] Polchinski and Strominger put forward a different proposal to circumvent the

mismatch of d.o.f. between the bosonic string model and the transverse oscillations. An effective string was built, with an action analogous to the Polyakov one, where the independent scale e^ϕ of the metric gets replaced by the induced metric. This model is certainly very interesting, and it is receiving nowadays a renewed attention [58, 48]. It is noticeable that the excitation spectra obtained within this model agree with the naïve NG ones up to two loops in the $1/(\sigma\mathcal{A})$ expansion; the prediction of this model would therefore nicely agree with NG in the region where the latter is valid. Higher corrections, whose computation does not appear to be simple, could in principle better explain the data for smaller lattices.

In conclusion, there is a renewed interest in the problem of identifying the correct QCD string dual and of testing the various proposals, see for instance [19, 58–60, 48, 61]. As already said, our contribution corroborates the "experimental" result that the naïve treatment of the NG model provides a very accurate description of fluctuating surfaces for sufficiently large sizes, and that clear deviations appear for smaller lattices which should be accounted for by the correct dual model (at least down to some lower scale where the string description itself breaks down). On the theoretical side, our derivation of the exact partition function, and not just of its perturbative expansion, could offer some insight for a similar treatment of consistent models including also the extra d.o.f. arising in $d \neq 26$, or of the Polchinski-Strominger string.

Acknowledgments

A. Loop expansion of the exact result

As discussed in section 2 eq. (2.23), the exact expression of the interface partition function

$$\mathcal{I}^{(d)} = 2 \left(\frac{\sigma}{2\pi}\right)^{\frac{d-2}{2}} V_T \sqrt{\sigma\mathcal{A}u} \sum_{m=0}^{\infty} \sum_{k=0}^{m} c_k c_{m-k} \left(\frac{\mathcal{E}}{u}\right)^{\frac{d-1}{2}} K_{\frac{d-1}{2}}(\sigma\mathcal{A}\mathcal{E}) \qquad (A.1)$$

has to be expanded for large $\sigma\mathcal{A}$, in order to compare it with the result of the functional integral approach. Therefore we have to use the asymptotic expression eq. (3.3) of the modified Bessel functions for large argument which reads, making explicit the first coefficients $a_1^{(j)}$ and $a_2^{(j)}$,

$$K_j(z) \sim \sqrt{\frac{\pi}{2z}} e^{-z} \left\{ 1 + \frac{4j^2 - 1}{8z} + \frac{(4j^2 - 1)(4j^2 - 9)}{2!(8z)^2} + ... \right\} .$$

Inserting the expansion of Bessel functions in eq. (A.1) gives eq. (3.4) (which we repeat here for commodity):

$$\mathcal{I}^{(d)} = \sqrt{2\pi} \left(\frac{\sigma}{2\pi}\right)^{\frac{d-2}{2}} V_T \sum_{k,k'=0}^{\infty} c_k c_{k'} \left(\frac{\mathcal{E}}{u}\right)^{\frac{d-2}{2}} e^{-\sigma\mathcal{A}\mathcal{E}} \left(1 + \sum_{r=1}^{\infty} a_r^{(\frac{d-1}{2})} (\sigma\mathcal{A}\mathcal{E})^{-r} \right) . \qquad (A.2)$$

The expression of $\mathcal{E}$ was given in eq. (2.21), and can be rewritten as

$$\mathcal{E}(a,b) = \sqrt{1 + \frac{4\pi\,u}{\sigma\mathcal{A}}a + \frac{4\pi^2\,u^2}{(\sigma\mathcal{A})^2}b^2}$$

in terms of a and b defined as in eq. (3.6):

$$a = k + k' - \frac{d-2}{12}\;, \quad b = k - k'\;. \tag{A.3}$$

We expand $\mathcal{E}$ as:

$$\mathcal{E}(a,b) \sim 1 + \frac{u}{\sigma\mathcal{A}}2\pi a + \frac{u^2}{(\sigma\mathcal{A})^2}2\pi^2\left(b^2 - a^2\right) + \frac{u^3}{(\sigma\mathcal{A})^3}4\pi^3 a\left(a^2 - b^2\right) + \dots$$

and insert this expansion into eq. (A.2), obtaining

$$\mathcal{I}^{(d)} \propto \sigma^{\frac{d-2}{2}}\frac{e^{-\sigma\mathcal{A}}}{u^{\frac{d-2}{2}}} \sum_{k,k'=0}^{\infty} c_k c_{k'} e^{-2\pi u\left(k+k'-\frac{d-2}{12}\right)}$$

$$\times \left\{1 + \frac{u}{\sigma\mathcal{A}}(d-2)\pi a + \frac{u^2}{(\sigma\mathcal{A})^2}(d-2)\left[(d-6)\frac{\pi^2}{2}a^2 + \pi^2 b^2\right] + \mathcal{O}\left(\frac{1}{(\sigma\mathcal{A})^4}\right)\right\}$$

$$\times \left\{1 + \frac{u^2}{\sigma\mathcal{A}}2\pi^2\left(a^2 - b^2\right) - \frac{4\pi^3 u^3 a\left(a^2 - b^2\right) - 2\pi^4 u^4\left(b^2 - a^2\right)^2}{(\sigma\mathcal{A})^2} + \mathcal{O}\left(\frac{1}{(\sigma\mathcal{A})^3}\right)\right\}$$

$$\times \left\{1 + \frac{1}{\sigma\mathcal{A}}\frac{d(d-2)}{8} - \frac{\frac{d(d-2)(d^2-2d-8)}{128} - \frac{\pi u\,d(d-2)a}{4}}{(\sigma\mathcal{A})^2} + \mathcal{O}\left(\frac{1}{(\sigma\mathcal{A})^3}\right)\right\}\;.$$

The result up to the third order is thus of the form of eq. (3.8):

$$\mathcal{I}^{(d)} \propto \sigma^{\frac{d-2}{2}}\frac{e^{-\sigma\mathcal{A}}}{u^{\frac{d-2}{2}}} \sum_{k,k'=0}^{\infty} c_k c_{k'} e^{-2\pi u\left(k+k'-\frac{d-2}{12}\right)} \left\{1 + \frac{g_1}{\sigma\mathcal{A}} + \frac{g_2}{(\sigma\mathcal{A})^2}\right\}\;, \tag{A.4}$$

with g_1 and g_2 explicitly given by

$$g_1 = \frac{d(d-2)}{8} + u(d-2)\pi a - u^2 2\pi^2\left(b^2 - a^2\right)\;, \tag{A.5}$$

$$g_2 = \left[\frac{d(d-2)(d^2-2d-8)}{128}\right] + u\frac{d(d-2)(d-4)\pi}{8}a + u^2\frac{(d-2)(d-4)\pi^2}{4}\left(3a^2 - b^2\right)$$

$$+ u^3 2\pi^3(d-4)a\left(a^2 - b^2\right) + u^4 2\pi^4\left(b^2 - a^2\right)^2\;. \tag{A.6}$$

Introducing the new variable $Q = \exp(-2\pi u)$ we can write eq. (A.4) in the form

$$\mathcal{I}^{(d)} \propto \sigma^{\frac{d-2}{2}}\frac{e^{-\sigma\mathcal{A}}}{u^{\frac{d-2}{2}}} \lim_{\overline{Q}\to Q} \left\{1 + \frac{g_1}{\sigma\mathcal{A}} + \frac{g_2}{(\sigma\mathcal{A})^2}\right\}\left[\eta(Q)\eta(\overline{Q})\right]^{2-d}\;, \tag{A.7}$$

where we have replaced a and b with the derivatives on Q and $\overline{Q}$ (see eq. (3.10)):

$$a \to Q\frac{d}{dQ} + \overline{Q}\frac{d}{d\overline{Q}}\;, \tag{A.8}$$

$$b \to Q\frac{d}{dQ} - \overline{Q}\frac{d}{d\overline{Q}}\;. \tag{A.9}$$

– 20 –

As we can see from the expansion coefficients (A.5) and (A.6), the only terms involving powers of a and b higher than 1 are

$$b^2 - a^2 = -4Q\frac{d}{dQ}\overline{Q}\frac{d}{d\overline{Q}}$$

$$3a^2 - b^2 = 2\left(Q\frac{d}{dQ}\right)^2 + 2\left(\overline{Q}\frac{d}{d\overline{Q}}\right)^2 + 8Q\frac{d}{dQ}\overline{Q}\frac{d}{d\overline{Q}}$$

$$\left(b^2 - a^2\right)^2 = 16\left(Q\frac{d}{dQ}\right)^2\left(\overline{Q}\frac{d}{d\overline{Q}}\right)^2$$

which have to be applied to $\eta^{2-d}(Q)\eta^{2-d}(\overline{Q})$. Applying the expressions eq. (C.8) and eq. (C.9) of the first logarithmic derivatives of the eta-function given in Appendix C, we have

$$Q\frac{d}{dQ}\eta^{2-d}(Q) = (2-d)\eta^{2-d}(Q)\frac{E_2(Q)}{24} ,$$

$$\left(Q\frac{d}{dQ}\right)^2\eta^{2-d}(Q) = (2-d)\eta^{2-d}(Q)\frac{(4-d)E_2^2(Q) - 2E_4(Q)}{576} .$$

It is easy to check that, after the application of the derivatives, a factor of $\eta^{4-2d}(iu)$ will always appear in front of the various terms and the total result up to the third order can be written in the following form:

$$\mathcal{I}^{(d)} \propto \sigma^{\frac{d-2}{2}}\frac{e^{-\sigma\mathcal{A}}}{u^{\frac{d-2}{2}}}\frac{1}{\eta^{2d-4}(iu)}\left\{1 + \frac{f_1}{\sigma\mathcal{A}} + \frac{f_2}{(\sigma\mathcal{A})^2}\right\} .$$

First of all we consider the f_1 term derived from the g_1 one. As one can see, the only derivative involved in the computation is $Q\frac{d}{dQ}$: this implies that our final formula will include E_2 functions but no E_4. We can divide the calculation in function of the powers of u. The term independent from it is the first one appearing in eq. (A.5):

$$f_{1,0} = \frac{d(d-2)}{8}.$$

The next power of u, after the substitution (A.8), gives, acting on the η functions,

$$f_{1,1} = -2\pi u(d-2)^2\frac{E_2(iu)}{24}.$$

The last term is instead:

$$f_{1,2} = 2\pi^2 u^2(d-2)^2\frac{E_2^2(iu)}{144}.$$

The final result is:

$$f_1 = \left\{\frac{(d-2)^2}{2}\left[\left(\frac{\pi}{6}\right)^2 u^2 E_2^2(iu) - \frac{\pi}{6}uE_2(iu)\right] + \frac{d(d-2)}{8}\right\} . \tag{A.10}$$

Proceeding in the same way to evaluate f_2 we find:

$$
\begin{aligned}
f_2 = \Bigg\{ & u^4 \frac{\pi^4 (d-2)^2}{18} \left[\frac{(4-d)E_2^2 - 2E_4}{24} \right]^2 + u^3 \frac{\pi^3}{72} (d-4)(d-2)^2 \left[\frac{E_2^3}{12} (4-d) \right. \\
& \left. - \frac{E_2 E_4}{6} \right] + u^2 \frac{\pi^2 (d-2)^2 (d-4)}{4} \left[\frac{E_4}{72} + \frac{(3d-8)E_2^2}{144} \right] \\
& - u \frac{\pi}{96} d(d-2)^2 (d-4) E_2 + \frac{1}{128} d(d-2)(d^2 - 2d - 8) \Bigg\}
\end{aligned}
\tag{A.11}
$$

(all modular forms above have to be evaluated at iu).

B. The two loop contribution: functional integral computation

In this appendix we check the calculation of the two-loop terms of the free energy made by Dietz and Filk with the functional integral method. Starting from the partition function written in the physical gauge and expanding it in powers of $\frac{1}{\sigma \mathcal{A}}$, one can evaluate it on a rectangular domain B of sizes (R, T). Defining $\mathbf{G}$ as the inverse Laplacian of the theory, the second order terms are given, in the notation of [29], by:

$$
\begin{aligned}
Z_{\Gamma, B}^{(2)} = \Big[& \lambda_1 D(D-1)(\langle 1 \rangle - \langle 2 \rangle) + \lambda_2 D(\langle 3 \rangle + \langle 4 \rangle + 2\langle 1 \rangle - 4\langle 2 \rangle) \\
& + \frac{\lambda_2}{3} D(D-1)(\langle 3 \rangle + \langle 4 \rangle + 6\langle 1 \rangle) \Big] ,
\end{aligned}
\tag{B.1}
$$

where D is $d-2$ in our notation, Γ speficies the specifiesof the boundary B; we are interested in the case where the topology is $S_1 \times S_1$. λ_1 and λ_2 are parameters which depend on the string model under consideration and in particular they are given by

$$
\lambda_1 = 1, \quad \lambda_2 = -\frac{1}{4}
\tag{B.2}
$$

in the Nambu-Goto case. Moreover, the following definitions are used:

$$
\begin{aligned}
\langle 1 \rangle &= \frac{1}{\sigma} \int_0^R dz \int_0^T dt \frac{\partial^2 \mathbf{G}}{\partial z \partial z'}\Big|_{z=z', t=t'} \frac{\partial^2 \mathbf{G}}{\partial t \partial t'}\Big|_{z=z', t=t'} , \\
\langle 2 \rangle &= \frac{1}{\sigma} \int_0^R dz \int_0^T dt \left(\frac{\partial^2 \mathbf{G}}{\partial z \partial t'} \right)^2 \Big|_{z=z', t=t'} , \\
\langle 3 \rangle &= \frac{3}{\sigma} \int_0^R dz \int_0^T dt \left(\frac{\partial^2 \mathbf{G}}{\partial z \partial z'} \right)^2 \Big|_{z=z', t=t'} , \\
\langle 4 \rangle &= \frac{3}{\sigma} \int_0^R dz \int_0^T dt \left(\frac{\partial^2 \mathbf{G}}{\partial t \partial t'} \right)^2 \Big|_{z=z', t=t'} .
\end{aligned}
$$

Notice that the formulæused by Dietz and Filk in eq. (3.4) have to be multiplied by $-\frac{1}{2}$ to get the right normalization of their final result eq. (3.7).

We shall deal with the divergent terms within the ζ-function regularization scheme, following Dietz and Filk. In the Nambu-Goto model with $S_1 \times S_1$ boundary conditions on

the rectangular domain, the Green function is:

$$\mathbf{G} = \frac{1}{4\pi^2 RT} \sum_{\substack{m,n=-\infty \\ (m,n)\neq(0,0)}}^{+\infty} \frac{\exp\left\{2\pi\mathrm{i}\frac{m}{T}(t-t')\right\}\exp\left\{2\pi\mathrm{i}\frac{n}{R}(z-z')\right\}}{\frac{n^2}{R^2}+\frac{m^2}{T^2}} \ .$$

Let us now evaluate the various terms of $Z^{(2)}_{S_1\times S_1,(R,T)}$. To begin with, we find

$$\langle 1 \rangle = \frac{1}{\sigma RT} \sum_{\substack{m,n,p,q=-\infty \\ (m,n)\neq(0,0) \\ (p,q)\neq(0,0)}}^{+\infty} \frac{\frac{n^2}{R^2}\frac{q^2}{T^2}}{\left(\frac{n^2}{R^2}+\frac{m^2}{T^2}\right)\left(\frac{p^2}{R^2}+\frac{q^2}{T^2}\right)}$$

$$= \frac{1}{\sigma RT}\left[16\sum_{m,n,p,q=1}^{+\infty}\frac{\frac{n^2}{R^2}\frac{q^2}{T^2}}{\left(\frac{n^2}{R^2}+\frac{m^2}{T^2}\right)\left(\frac{p^2}{R^2}+\frac{q^2}{T^2}\right)} + (m=0,n\neq0,p,q)\right.$$

$$\left. + (m,n,p=0,q\neq0) - (m=0,n\neq0,p=0,q\neq0)\right] \ , \tag{B.3}$$

where with $(m=0,n\neq0,p,q)$ we indicate the sum over any n different from zero, any p and any q when m has been fixed at zero. The last term in r.h.s. of eq. (B.3) is to avoid the double counting and the first one can be rewritten using the equality

$$\sum_{m,n=1}^{\infty}\frac{\frac{n^2}{R^2}}{\frac{n^2}{R^2}+\frac{m^2}{T^2}} = E_2\left(\mathrm{i}\frac{R}{T}\right)\frac{\pi}{24}\frac{R}{T} \ . \tag{B.4}$$

The result is

$$\langle 1 \rangle = \frac{1}{\sigma RT}\left[\left(\frac{\pi}{6}\right)^2 E_2\left(\mathrm{i}\frac{R}{T}\right)E_2\left(\mathrm{i}\frac{T}{R}\right) + (m=0,n\neq0,p,q)\right.$$

$$\left. + (m,n,p=0,q\neq0) - (m=0,n\neq0,p=0,q\neq0)\right] \ .$$

The last three terms can be evaluated using (B.4) and the ζ function regularization and they sum up to

$$-\frac{\pi}{6}\frac{R}{T}E_2\left(\mathrm{i}\frac{R}{T}\right) - \frac{\pi}{6}\frac{T}{R}E_2\left(\mathrm{i}\frac{T}{R}\right) + 1 \ ,$$

which vanishes using the modular property (C.6) for the Eisenstein series E_2. We get thus

$$\langle 1 \rangle = \frac{1}{\sigma RT}H \ ,$$

where we have defined for notational convenience

$$H = \left(\frac{\pi}{6}\right)^2 E_2\left(\mathrm{i}\frac{T}{R}\right)E_2\left(\mathrm{i}\frac{R}{T}\right) \ . \tag{B.5}$$

The contribution $\langle 2 \rangle$ vanishes because the terms in the sum are odd:

$$\langle 2 \rangle = \frac{1}{\sigma RT}\sum_{\substack{m,n,p,q=-\infty \\ (m,n)\neq(0,0) \\ (p,q)\neq(0,0)}}^{+\infty}\frac{mnpq}{\left(\frac{n^2}{R^2}+\frac{m^2}{T^2}\right)\left(\frac{p^2}{R^2}+\frac{q^2}{T^2}\right)} = 0 \ .$$

To compute the expression $(\langle 3 \rangle + \langle 4 \rangle + 6\langle 1 \rangle)$ which appears in (B.1), one can rewrite it as a perfect square:

$$(\langle 3 \rangle + \langle 4 \rangle + 6\langle 1 \rangle) = \frac{3}{\sigma} \int_0^R dz \int_0^T dt \left(\frac{\partial^2 \mathbf{G}}{\partial z \partial z'} + \frac{\partial^2 \mathbf{G}}{\partial t \partial t'} \right)^2 \Big|_{z=z', t=t'}$$

$$= \frac{3}{\sigma RT} \left[\sum_{\substack{m,n=-\infty \\ (m,n)\neq(0,0)}}^{+\infty} \frac{\frac{n^2}{R^2} + \frac{m^2}{T^2}}{\frac{n^2}{R^2} + \frac{m^2}{T^2}} \right]^2 = \frac{3}{\sigma RT} \ .$$

Collecting the previous results we obtain the following system of equations:

$$\langle 1 \rangle = \frac{H}{\sigma RT} \ ,$$
$$\langle 2 \rangle = 0 \ ,$$
$$\langle 3 \rangle + \langle 4 \rangle + 6\langle 1 \rangle = \frac{3}{\sigma RT}$$

which gives, for the last term in equation (B.1):

$$\langle 3 \rangle + \langle 4 \rangle + 2\langle 1 \rangle - 4\langle 2 \rangle = \frac{3 - 4H}{\sigma RT} \ .$$

The total second order correction is therefore

$$Z_{S_1 \times S_1, B} = \frac{1}{\sigma RT} \left\{ D(D-1)H - \frac{1}{4}D(3 - 4H) - \frac{3}{12}D(D-1) \right\}$$

$$= \frac{1}{\sigma RT} \left\{ D^2 H - \frac{1}{4}D(D+2) \right\} \ . \tag{B.6}$$

This corresponds to our result[8] eq. (A.10) where $D = d - 2$, up to an overall factor of $-\frac{1}{2}$.

C. Useful formulæ

In this appendix we collect some useful formulæ.

Dedekind η function. The Dedekind eta function is defined, in terms of the quantity $q = \exp\{2\pi i \tau\}$, by

$$\eta(\tau) = q^{\frac{1}{24}} \prod_{n=1}^{\infty} (1 - q^n) \ . \tag{C.1}$$

One can expand it in q-series:

$$[\eta(\tau)]^{-1} = \sum_{k=0}^{\infty} p_k \, q^{k-\frac{1}{24}} \ , \tag{C.2}$$

where p_k's are the number of partitions of k. In the text, we often switch between the notation $\eta(\tau)$ and $\eta(q)$ for the function defined in eqs. (C.1), (C.2), according to the convenience.

---

[8]Dietz and Filk found: $Z^{(2)}_{S_1 \times S_1, (R,T)} = \frac{1}{\sigma RT} \left\{ D^2 H - \frac{1}{4}[D(4D-1)] \right\}$

Under the modular transformations T and S the Dedekind eta function transforms in the following way:

$$\eta(\tau + 1) = e^{\frac{i\pi}{12}}\eta(\tau) \ , \tag{C.3}$$

$$\eta(-\frac{1}{\tau}) = (e^{-i\frac{\pi}{2}}\tau)^{\frac{1}{2}}\eta(\tau) \ . \tag{C.4}$$

Eisenstein series. The second Eisenstein function is defined by

$$E_2(\tau) = 1 - 24\sum_{n=1}^{\infty}\sigma_1(n)q^n = 1 - 24\sum_{k=1}^{\infty}\frac{kq^k}{1-q^k} \ ,$$

where $\sigma_1(n)$ denotes the sum of the positive divisors of n. An useful property is

$$q\frac{d}{dq}E_2(\tau) = \frac{E_2^2(\tau) - E_4(\tau)}{12} \ . \tag{C.5}$$

where the fourth Eisenstein series is defined, in terms of the sum of the cubes of the positive divisors of n, $\sigma_3(n)$, as

$$E_4(\tau) = 1 + 240\sum_{n=1}^{+\infty}\sigma_3(n)\,q^n \ .$$

The modular properties of the Eisenstein functions are:

$$E_2(\tau) = \left(\frac{1}{\tau}\right)^2 E_2\left(-\frac{1}{\tau}\right) + \frac{6}{\pi}\frac{i}{\tau} \ , \tag{C.6}$$

$$E_{2k}(\tau) = (-1)^k\left(\frac{1}{\tau}\right)^{2k}E_{2k}\left(-\frac{1}{\tau}\right), k \geq 2 \ . \tag{C.7}$$

Multiple logarithmic derivatives of the eta function are related to Eisenstein series, and in particular we have:

$$q\frac{d}{dq}\eta^\alpha(\tau) = \alpha\eta^\alpha(\tau)\frac{E_2(\tau)}{24} \ , \tag{C.8}$$

$$\left(q\frac{d}{dq}\right)^2\eta^\alpha(\tau) = \alpha\eta^\alpha\frac{(\alpha+2)E_2(\tau)^2 - 2E_4(\tau)}{576} \ . \tag{C.9}$$

Poisson resummation formula. In section 2 the following resummation formula plays a key role:

$$\sum_{n=-\infty}^{+\infty}\exp\{-\pi an^2 + 2\pi ibn\} = a^{-\frac{1}{2}}\sum_{m=-\infty}^{+\infty}\exp\left\{-\frac{\pi(m-b)^2}{a}\right\} . \tag{C.10}$$

References

[1] K.G. Wilson, *Confinement of quarks, Phys. Rev.* **D 10** (1974) 2445;
S. Mandelstam, *Vortices and quark confinement in nonabelian gauge theories, Phys. Rept.* **23** (1976) 245;
H.B. Nielsen and P. Olesen, *Vortex-line models for dual strings, Nucl. Phys.* **B 61** (1973) 45;

G. 't Hooft, *A two-dimensional model for mesons*, *Nucl. Phys.* **B 75** (1974) 461;
A.M. Polyakov, *String representations and hidden symmetries for gauge fields*, *Phys. Lett.* **B 82** (1979) 247; *Gauge fields as rings of glue*, *Nucl. Phys.* **B 164** (1980) 171;
Y. Nambu, *QCD and the string model*, *Phys. Lett.* **B 80** (1979) 372.

[2] M. Lüscher, K. Symanzik and P. Weisz, *Anomalies of the free loop wave equation in the wkb approximation*, *Nucl. Phys.* **B 173** (1980) 365.

[3] M. Lüscher, *Symmetry breaking aspects of the roughening transition in gauge theories*, *Nucl. Phys.* **B 180** (1981) 317.

[4] P. Olesen, *Strings and QCD*, *Phys. Lett.* **B 160** (1985) 144.

[5] M. Lüscher and P. Weisz, *Locality and exponential error reduction in numerical lattice gauge theory*, *JHEP* **09** (2001) 010 [`hep-lat/0108014`].

[6] M. Caselle, R. Fiore, F. Gliozzi, M. Hasenbusch and P. Provero, *String effects in the Wilson loop: a high precision numerical test*, *Nucl. Phys.* **B 486** (1997) 245 [`hep-lat/9609041`].

[7] P. de Forcrand, M. D'Elia and M. Pepe, *A study of the 't Hooft loop in* SU(2) *Yang-Mills theory*, *Phys. Rev. Lett.* **86** (2001) 1438 [`hep-lat/0007034`];
M. Pepe and P. De Forcrand, *Finite-size scaling of interface free energies in the 3D ising model*, *Nucl. Phys.* **106** *(Proc. Suppl.)* (2002) 914 [`hep-lat/0110119`].

[8] M. Caselle, M. Hasenbusch and M. Panero, *String effects in the 3D gauge ising model*, *JHEP* **01** (2003) 057 [`hep-lat/0211012`].

[9] M. Lüscher and P. Weisz, *Quark confinement and the bosonic string*, *JHEP* **07** (2002) 049 [`hep-lat/0207003`].

[10] M. Lüscher and P. Weisz, *String excitation energies in* SU(N) *gauge theories beyond the free-string approximation*, *JHEP* **07** (2004) 014 [`hep-th/0406205`].

[11] M. Caselle, M. Hasenbusch and M. Panero, *Short distance behaviour of the effective string*, *JHEP* **05** (2004) 032 [`hep-lat/0403004`].

[12] M. Caselle, M. Pepe and A. Rago, *Static quark potential and effective string corrections in the (2+1)-D* SU(2) *Yang-Mills theory*, *JHEP* **10** (2004) 005 [`hep-lat/0406008`].

[13] M. Caselle, M. Hasenbusch and M. Panero, *Comparing the Nambu-Goto string with LGT results*, *JHEP* **03** (2005) 026 [`hep-lat/0501027`].

[14] M. Caselle, M. Hasenbusch and M. Panero, *On the effective string spectrum of the tridimensional* Z_2 *gauge model*, *JHEP* **01** (2006) 076 [`hep-lat/0510107`].

[15] P. de Forcrand and D. Noth, *Precision lattice calculation of* SU(2) *'t Hooft loops*, *Phys. Rev.* **D 72** (2005) 114501 [`hep-lat/0506005`].

[16] F. Bursa and M. Teper, *Casimir scaling of domain wall tensions in the deconfined phase of D = 3+1* SU(N) *gauge theories*, *JHEP* **08** (2005) 060 [`hep-lat/0505025`].

[17] K.J. Juge, J. Kuti and C. Morningstar, *Fine structure of the QCD string spectrum*, *Phys. Rev. Lett.* **90** (2003) 161601 [`hep-lat/0207004`].

[18] K.J. Juge, J. Kuti and C. Morningstar, *The casimir energy paradox of the QCD string*, *Nucl. Phys.* **129** *(Proc. Suppl.)* (2004) 686 [`hep-lat/0310039`].

[19] K.J. Juge, J. Kuti and C. Morningstar, *QCD string formation and the Casimir energy*, `hep-lat/0401032`.

[20] S. Necco and R. Sommer, *The $N_f = 0$ heavy quark potential from short to intermediate distances*, *Nucl. Phys.* **B 622** (2002) 328 [`hep-lat/0108008`].

[21] B. Lucini and M. Teper, *Confining strings in* SU(N) *gauge theories*, *Phys. Rev.* **D 64** (2001) 105019 [`hep-lat/0107007`].

[22] P. Majumdar, *The string spectrum from large Wilson loops*, *Nucl. Phys.* **B 664** (2003) 213 [`hep-lat/0211038`].

[23] Y. Koma, M. Koma and P. Majumdar, *Static potential, force and flux-tube profile in 4D compact U(1) lattice gauge theory with the multi-level algorithm*, *Nucl. Phys.* **B 692** (2004) 209 [`hep-lat/0311016`].

[24] P. Majumdar, *Continuum limit of the spectrum of the hadronic string*, `hep-lat/0406037`.

[25] M. Panero, *A numerical study of confinement in compact QED*, *JHEP* **05** (2005) 066 [`hep-lat/0503024`].

[26] O. Jahn and P. de Forcrand, *Baryons and confining strings*, *Nucl. Phys.* **B 129** (2004) 700.

[27] O. Jahn and O. Philipsen, *The Polyakov loop and its relation to static quark potentials and free energies*, *Phys. Rev.* **D 70** (2004) 074504 [`hep-lat/0407042`].

[28] H. Meyer and M. Teper, *Confinement and the effective string theory in* $SU(n \to \infty)$: *a lattice study*, *JHEP* **12** (2004) 031 [`hep-lat/0411039`].

[29] K. Dietz and T. Filk, *On the renormalization of string functionals*, *Phys. Rev.* **D 27** (1983) 2944.

[30] Y. Nambu, in *Symmetries and quark models*, R. Chand ed., Gordon and Breach, New York, 1970;
T. Goto, *Relativistic quantum mechanics of one-dimensional mechanical continuum and subsidiary condition of dual resonance model*, *Prog. Theor. Phys.* **46** (1971) 1560;
Y. Nambu, *Strings, monopoles and gauge fields*, *Phys. Rev.* **D 10** (1974) 4262.

[31] O. Alvarez, *The static potential in string models*, *Phys. Rev.* **D 24** (1981) 440.

[32] J.F. Arvis, *The exact q $\bar{q}$ potential in Nambu string theory*, *Phys. Lett.* **B 127** (1983) 106.

[33] M. Billó and M. Caselle, *Polyakov loop correlators from D0-brane interactions in bosonic string theory*, *JHEP* **07** (2005) 038 [`hep-th/0505201`].

[34] M. Caselle, M. Hasenbusch and M. Panero, *High precision Monte Carlo simulations of interfaces in the three-dimensional ising model: a comparison with the Nambu-Goto effective string model*, `hep-lat/0601023`.

[35] M.P. Gelfand and M.E. Fisher, *Physica* **A 166** (1990) 1;
V. Privman, *Fluctuating interfaces, surface tension and capillary waves: an introduction*, *Int. J. Mod. Phys.* **C3** (1992) 857–877 [`cond-mat/9207003`].

[36] V. Privman, *Fluctuating interfaces, surface tension and capillary waves: an introduction*, *Int. J. Mod. Phys.* **C3** (1992) 857–877 [`cond-mat/9207003`].

[37] F. P. Buff, R. A. Lovett and F. H. Stillinger Jr., *Phys. Rev. Lett.* **15** (1965) 621.

[38] J. Rowlinson and S. Widom, *Molecular theory of capillarity*, Clarendon Press, 1982.

[39] G. Münster, *Interface tension in three-dimensional systems from field theory*, *Nucl. Phys.* **B 340** (1990) 559.

[40] P. Provero and S. Vinti, *The 2D effective field theory of interfaces derived from 3D field theory*, *Nucl. Phys.* **B 441** (1995) 562 [`hep-th/9501104`].

[41] P. Hoppe and G. Münster, *The interface tension of the three-dimensional Ising model in two loop order*, *Phys. Lett.* **A 238** (1998) 265 [`cond-mat/9708212`].

[42] M. Caselle et al., *Rough interfaces beyond the gaussian approximation*, *Nucl. Phys.* **B 432** (1994) 590 [`hep-lat/9407002`].

[43] M. Hasenbusch and K. Pinn, *The interface tension of the 3-dimensional Ising model in the scaling region*, *Physica A* **245** (1997) 366, [`cond-mat/9704075`].

[44] M. Caselle and K. Pinn, *On the universality of certain non-renormalizable contributions in two-dimensional quantum field theory*, *Phys. Rev.* **D 54** (1996) 5179 [`hep-lat/9602026`].

[45] J. Polchinski, *String Theory* vol. 1, Cambridge University Press, 1998.

[46] A.M. Polyakov, *Quantum geometry of bosonic strings*, *Phys. Lett.* **B 103** (1981) 207.

[47] M.B. Green, J.H. Schwarz, E. Witten, *Superstring Theory* vol. 1, Cambridge University Press, 1988.

[48] J. Kuti, *Lattice QCD and string theory*, *PoS* **LAT2005** (2005) 001 [`hep-lat/0511023`].

[49] M. Caselle, M. Hasenbusch and M. Panero, *Short distance behaviour of the effective string*, *JHEP* **05** (2004) 032 [`hep-lat/0403004`].

[50] P. Goddard and C.B. Thorn, *Compatibility of the dual pomeron with unitarity and the absence of ghosts in the dual resonance model*, *Phys. Lett.* **B 40** (1972) 235.

[51] R.C. Brower, *Spectrum generating algebra and no ghost theorem for the dual model*, *Phys. Rev.* **D 6** (1972) 1655.

[52] R. Marnelius, *The bosonic string in D < 26 with and without Liouville fields*, *Phys. Lett.* **B 172** (1986) 337.

[53] J. Polchinski, *Strings and QCD?*, `hep-th/9210045`.

[54] A.M. Polyakov, *String theory and quark confinement*, *Nucl. Phys.* **68** *(Proc. Suppl.)* (1998) 1 [`hep-th/9711002`].

[55] A.M. Polyakov, *The wall of the cave*, *Int. J. Mod. Phys.* **A 14** (1999) 645 [`hep-th/9809057`].

[56] J.M. Maldacena, *The large-N limit of superconformal field theories and supergravity*, *Adv. Theor. Math. Phys.* **2** (1998) 231 [`hep-th/9711200`].

[57] J. Polchinski and A. Strominger, *Effective string theory*, *Phys. Rev. Lett.* **67** (1991) 1681.

[58] J.M. Drummond, *Universal subleading spectrum of effective string theory*, `hep-th/0411017`.

[59] R.C. Brower, C.I. Tan and E. Thompson, *Probing the 5th dimension with the QCD string*, *Int. J. Mod. Phys.* **A 20** (2005) 4508 [`hep-th/0503223`].

[60] R.C. Brower, *String/gauge duality: (re)discovering the QCD string in AdS space*, *Acta Phys. Polon.* **B34** (2003) 5927 [`hep-th/0508036`].

[61] S. Dalley, *SU(N(c) → ∞) lattice data and degrees of freedom of the QCD string*, `hep-th/0512264`.